Int J Adv Manuf Technol (2015) 80:921–930
DOI 10.1007/s00170-015-7073-7

ORIGINAL ARTICLE

Precise alignment method of the large-scale crankshaft during non-circular grinding

Nanyan Shen[1] · **Jing Li**[1] · **Jun Ye**[1] · **Xiang Qian**[1] · **Haitao Huang**[2]

Received: 10 October 2014 / Accepted: 19 March 2015 / Published online: 10 April 2015

Abstract A large-scale crankshaft of internal-combustion engine is easy to bend and twist when clamped onto the grinding machine. The deviation of workpiece axis from its optimal machining axis has a significant influence on machining accuracy of angle, eccentric throw, and diameter and contour of the heavy crankshaft in non-circular grinding. To reduce the consumption of manual labor and setting-up time, an automatic alignment approach and apparatus is proposed and integrated into the non-circular grinder. The on-machine gauge senses X and Y components of deviation of crank journal axis and feed them back to the computerized numerical control system. The motor-driving steady rests based on slider-crank mechanism are controlled to compensate for the deviation. The algorithm with self-correcting ability for compensation value is employed to make up for the finite contact stiffness of workpiece and steady rest. The results of three alignment tests are compared, which demonstrates the better effect on alignment precision and efficiency of the self-correcting compensation.

Keywords Automatic alignment · Elastic deformation · On-machine measuring · Servo steady rest · Self-correcting compensation

✉ Jing Li
ian1982@shu.edu.cn

Haitao Huang
huanghaitao@smtw.com

[1] School of Mechatronic Engineering and Automation, Shanghai Key Laboratory of Intelligent Manufacturing and Robotics, Shanghai University, Shanghai 200072, China

[2] Shanghai Machine Tool Works Ltd., Shanghai 200093, China

1 Introduction

Non-circular grinding controls the rotation of workpiece and the transverse feed of grinding carriage to make grinding wheel always tangent with crankpin, which allows the precision processing of crank journals and crankpins in one clamping [1–3].

However, the low stiffness of crankshaft leads to bending and twist deformation when clamped onto the grinder, which deflects the workpiece axis from the optimal machining axis. The deformations have to be taken into account to reduce geometric error resulting from the difference between the actual and the optimal axis.

The crankshaft of automotive engine is required to meet high-precision tolerances and high-quality surface finish and topography. Several investigations on out-of-roundness of crankpin arising from the various rotating stiffness of crankshaft are conducted. Methods of calculating the deformations of crankpin due to grinding force at each rotating angle are proposed and thus roundness error can be pre-compensated through correcting the movement of grinding carriage [4, 5]. The position information of grinding wheel related to workpiece directly collected from CNC system of non-circular grinding machine with no additional sensors is used to evaluate the dynamic contour error [6].

Sensors are integrated into non-circular grinding machine, which offers many advantages for quality assurance and reduction of setting-up and machining time. Roundness error signal is extracted in frequency domain using a small-signal model of the V-block roundness measurement method and the fast Fourier transformation, with which the in situ roundness correction data was generated and implanted to the numerical programme [7]. Contour errors and out-of-tolerance can be detected by measuring the angle, diameter, and contour of workpiece in grinder and then grinding process can be

improved by optimizing rotating speed and feed rate [8]. An in-line inspection system using machine vision is developed to differentiate sub-micron level roughness change of the crankshaft surface to eliminate manual inspection in a mass production process [9].

The influence of system stiffness on out-of-roundness of crankpin grinding with an eccentric chuck is studied experimentally [10]. The experimental results indicate that the work supports are beneficial to enhancing system stiffness and thus decreasing the roundness errors of crankpins. A positioning system consisting of an optical measurement system and an active tailstock is presented. Based on this system, a precontrol strategy considering grinding force, system stiffness, control deviations, etc. is proposed to achieve the higher machining accuracy and less time consuming [3, 11]. The dynamic performance and the cutting stability of the crankshaft grinding machine are evaluated based on a 7 DOF lumped-mass model and then the design variables of the substructures in crankshaft grinder are optimized [12].

As the key part of the internal-combustion engine used in ship [13, 14], locomotive, and electric power equipment, the large-scale crankshafts are generally several meters in length and several tones in weight, which deform much greater than the crankshafts of automobile engines in non-circular grinding. Steady rests are always required for the alignment of workpiece and the increase of system stiffness [15].

Conventionally, the alignment process is manually operated and the efficiency heavily relies on operator's experience. This paper presents a closed-loop solution for automatic precise alignment in non-circular grinding of the large and heavy crankshaft. An automatic alignment system consisted of measuring instrument integrated in grinder and servo steady rests driven by motor is proposed. Due to the elastic deformation of support pads and the various stiffness of crankshaft, the relationship between the correction to displacements of support pads and the change in deviation of crank journal axis appears nonlinear. Here, a self-correcting method is employed to determine the compensation for deviation.

2 Automatic alignment system

The automatic alignment system integrated into non-circular grinding machine consists of measuring instrument and servo steady rests (see Fig. 1a). The measuring instrument shown in Fig. 1b is used to gauge the deviation of crank journal axis, which is composed of v-shaped height caliper, pen type displacement sensor, grating ruler, pneumatic cylinder, etc. The set of measuring instrument is installed at the front end of cantilever support fixed on grinding carriage so that it can move along X- and Z-axes direction to gauge each crank journal of crankshafts with the different crank radius. Height caliper is laid down slowly along Y-axis direction by pneumatic cylinder until the V-block holds the crank journal for measurement.

Composed of housing, the upper and lower support arms with support pads, rods, ball screws, servo motors, etc., the servo steady rest works as actuator to compensate for the deviation (see Fig. 1c) [16]. The ball screw translates rotational motion of servo motor to linear motion of rod which rotates the support arm around pivot O_S to change the position of support pads for compensating deviation.

Figure 2 shows the alignment process of crankshaft based on servo steady rests including two main steps. The first step toward compensation is to ensure the touch between crank journals and support pads by the option function "Travel to fixed stop with torque control" of SIEMENS 840D SL CNC system [17]. Using this function, the support arms will keep approaching to workpiece until the output torque of servo motors reaches the specified percentage of the maximum drive torque.

The following alignment process is conducted automatically through the software embedded in PCU (HMI) of CNC system [18]. The Y-component deviation is obtained by the feedback s_j of grating ruler from PLC of numerical control system. If the X-component deviation exists, it will rotate the height caliper around pivot O_H. Utilizing the readout l_j at the head of height caliper read by the pen type displacement sensor, the X-component deviation can be calculated by the ratio of distances from pivot O_H to each end of height caliper. And then deviation (ex_j, ey_j) of crank journal which is calculated on the basis of measured data l_j and s_j form PLC is used to determine its correction (dx_j, dy_j) in the next round of compensation. The displacements of rods for the upper and lower support arms are computed and transmitted to NCU of SIEMENS 840D SL for the correction of support arms' rotating angles. This process will be repeated to reduce the deviation gradually until the alignment result of workpiece is satisfied.

2.1 Calculation of the deviation of crank journal

The measuring principle of the deviation of crank journal is shown in Fig. 3 where O and O_j' denote the optimal and actual centers of crank journal, respectively, so that the distance $|OO_j'|$ between O and O_j' is the deviation of crank journal No. j; O_H denotes the pivot of height caliper and the pen type displacement sensor locates at position A of height caliper. When the V-block of height caliper holds the crank journal No. j, the distance s_j height caliper drops is read by grating ruler and the length l_j of arc intercepted by the rotating angle of height caliper at position A is gauged by pen type displacement sensor. When height caliper rotates

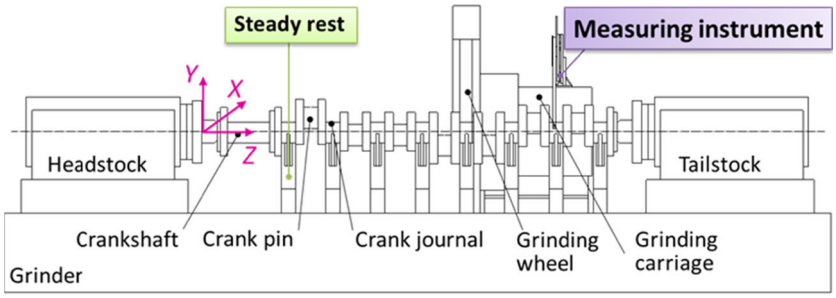

(a) Automatic alignment system integrated into non-circular grinding machine

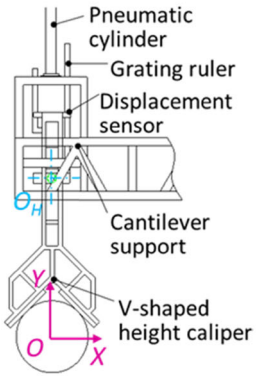

(b) Measuring instrument for gauging the deviation

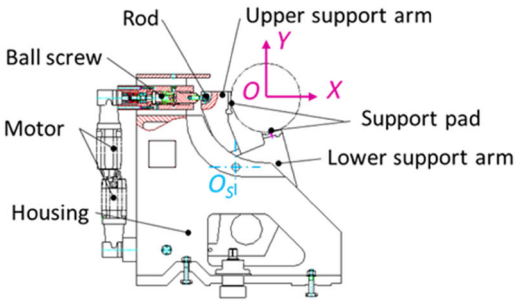

(c) Servo steady rest for compensating the deviation

Fig. 1 Hardware of automatic alignment system in non-circular grinding. **a** Automatic alignment system integrated into non-circular grinding machine. **b** Measuring instrument for gauging the deviation. **c** Servo steady rest for compensating the deviation

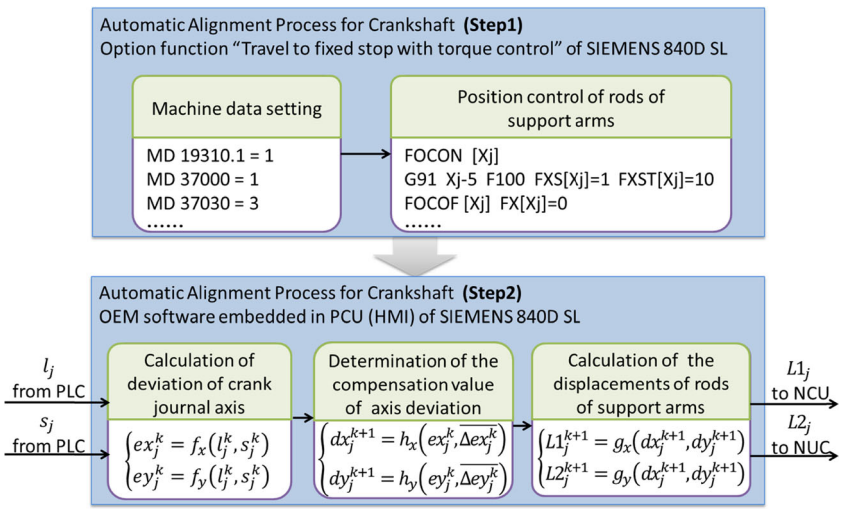

Fig. 2 Alignment process of crankshaft based on servo steady rests

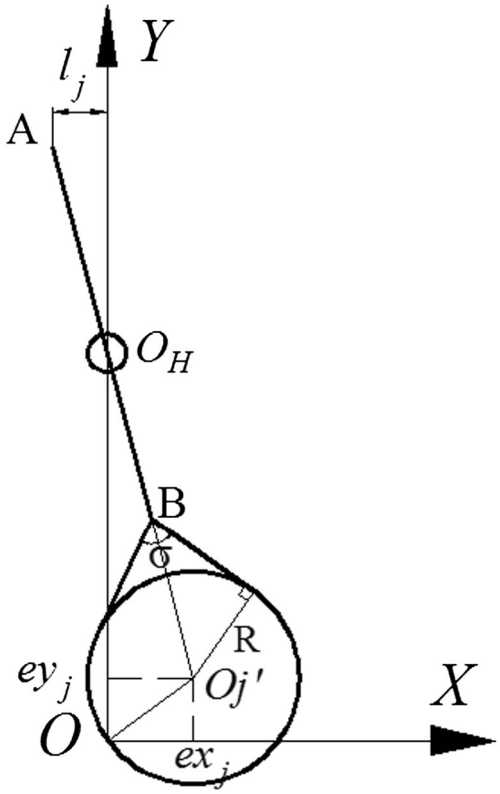

Fig. 3 Measuring principle of the deviation

clockwise around pivot O_H, the length l_j is a positive number; otherwise, it is negative.

The formulas for X and Y components of deviation are derived from the geometrical relations described in Fig. 3:

$$\begin{cases} ex_j = sign(-1 \times l_j)\cdot\sin\angle O_H O O_j'\cdot\left|OO_j'\right| \\ ey_j = \cos\angle O_H O O_j'\cdot\left|OO_j'\right| \end{cases} \tag{1}$$

In the last equation, the angle $\angle O_H O O_j'$ and the length of the side OO_j' of triangle $\Delta O O_H O_j'$ are presented by Eqs. (2) and (3) using the law of cosines.

$$\angle O_H O O_j' = \cos^{-1}\left(\frac{|O_H O|^2 + \left|OO_j'\right|^2 - \left|O_H O_j'\right|^2}{2\cdot|O_H O|\cdot\left|OO_j'\right|}\right) \tag{2}$$

$$\left|OO_j'\right| = \sqrt{\left|O_H O_j'\right|^2 + |O_H O|^2 - 2\cdot\left|O_H O_j'\right|\cdot|O_H O|\cdot\cos\angle O O_H O_j'} \tag{3}$$

where the angle $\angle O O_H O_j'$ in radians approximately equals to the ratio of the lengths of l_j and AO_H as Eq. (4) for the reason that the length of l_j is much less than that of AO_H; the height of pivot O_H at the current position equals to the difference of its initial height H_0 and s_j as Eq. (5); the length of side $O_H O_j'$ is the distance between the crank journal's center O_j' and the current position of pivot O_H expressed by Eq. (6).

$$\angle O O_H O_j' \approx \frac{|l_j|}{|AO_H|} \tag{4}$$

$$|O_H O| = H_0 - s_j \tag{5}$$

$$\left|O_H O_j'\right| = |O_H B| + \left|B O_j'\right| = |O_H B| + \frac{R}{\cos(\sigma/2)} \tag{6}$$

Where the lengths of $O_H A$ and $O_H B$, the radius of crank journal R and the included angle of V-block are known by calibrating the height caliper.

Thus, X and Y components of deviation are solved by substituting Eqs. (2) and (3) for $\angle O_H O O_j'$ and $|OO_j'|$ in Eq. (1), respectively.

2.2 Calculation of the displacements of rods of support arm

The slider-crank mechanism used in the design of support arm is shown in Fig. 4. The parameters used to define the angles and the link lengths of the upper support arm are given: the angles $EO_S S$, $GO_S B$, $BO_S M$ and the lengths of links $O_S E$, $O_S G$, $O_S A$, $O_S B$, $O_S M$ are equal to ψ_1, θ_1, γ_1 and l_{11}, l_{12}, l_{13}, l_{14}, l_{15}. Similarly, the angles $FO_S T$, $HO_S C$, and $CO_S P$ of the lower support arm are defend as ψ_2, θ_2, and γ_2; the lengths of links $O_S F$, $O_S H$, $O_S C$, $O_S D$, and $O_S P$ as l_{21}, l_{22}, l_{23}, l_{24}, and l_{25}. The upper and lower support arms share the pivot O_S. Taking the lower support arm for example, link $O_S F$ is fixed so that the mechanism converts the reciprocating motion of link FH (namely rod) into the oscillating motion of link $O_S H$ (namely support arm).

Based on the mechanism geometry shown in Fig. 4, kinematic analysis of the lower support arm is investigated with the known deviation of crank journal. Link $O_S P$ is perpendicular to the bottom side CD of support pad and intersects the extended line of top side $C'D'$ at point Q. Without any consideration for the elastic deformation of support pad w_2 wide and h_2 high, the crank journal contacts with the top side $C'D'$ at point K. In $UO_S V$ coordinates, the angle of link $O_S H$ is determined by finding the angle σ_2 contained between the top side $C'D'$ of support pad and the positive direction of U axis. Moving the origin O to point O_S, the coordinates XOY translates to $UO_S V$. And coordinates values of center O of headstock is (U_O, V_O) which defines its position on coordinate plane $UO_S V$.

Let the equation of line KQ be $v = k_2 \cdot u + b_2$. Thus, simultaneous Eq. (7) can be found because line KQ is the common tangents of circle O' and circle O_S.

$$\begin{cases} \left|k_2\cdot u_{O'} - b_2 - v_{O'}\right| = R\cdot\sqrt{1+k_2^2} \\ |b_2| = (l_{25}+h_2)\cdot\sqrt{1+k_2^2} \end{cases} \tag{7}$$

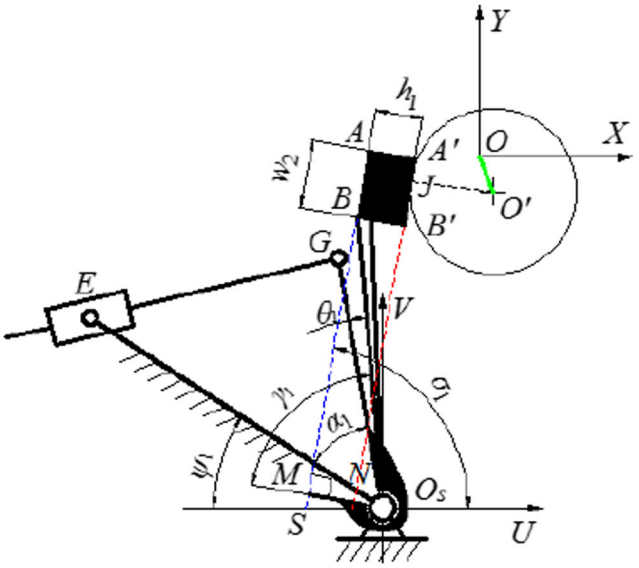

(a) The upper support arm

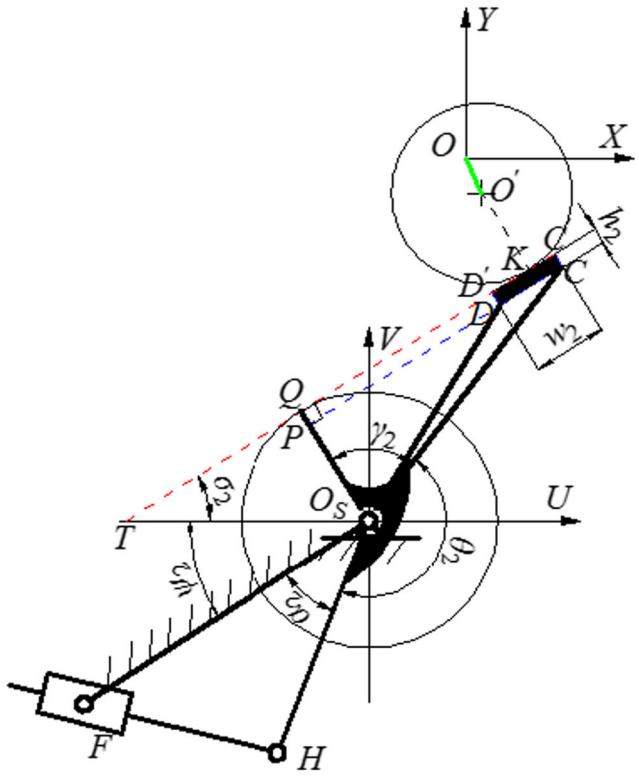

(b) The lower support arm

Fig. 4 Slider-crank mechanism of support arm. **a** The upper support arm. **b** The lower support arm

Where $(u_{O'}, v_{O'})$ denotes the coordinates values of the actual crank journal's center O' on coordinate plane UO_SV.

Four sets of values for k_2 and b_2 representing two external tangents and two internal tangents could be found by solving the simultaneous equations. None but the set of values representing the internal tangent shown in Fig. 5 is the feasible solution. Additionally, find the contact point K by solving the

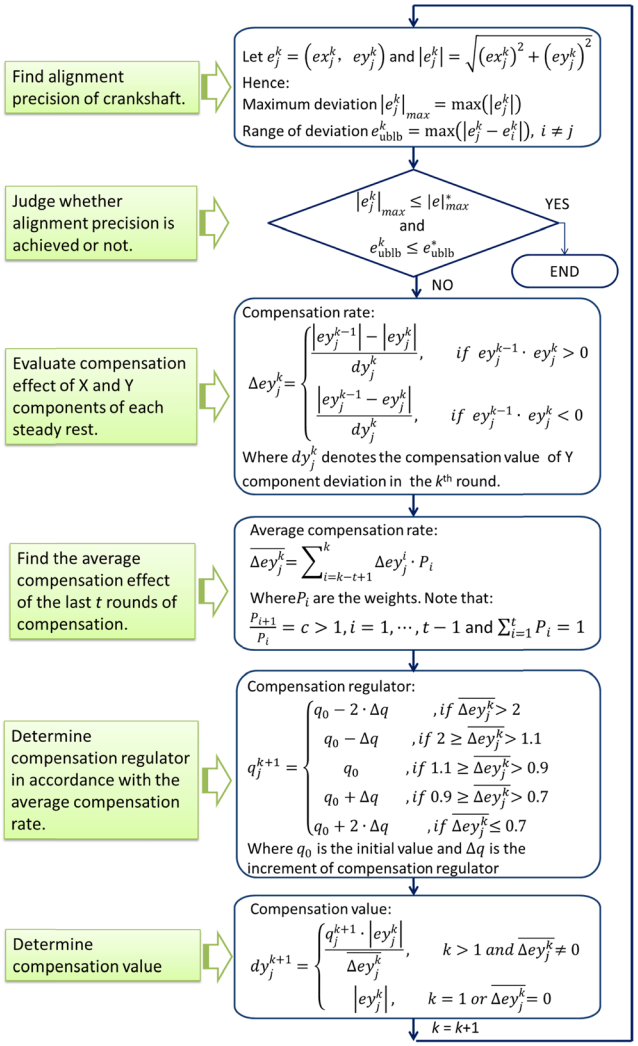

Fig. 5 Flowchart of the algorithm for determining compensation value

simultaneous equations of tangent KQ and circle O' and then verify whether it locates between points C' and D' on the top side of support pad. If contact point K lies at the extended line of side $C'D'$, it indicates that the width or height of the support pad in usage does not match to the radius of crank journal.

Angle $\angle FO_SH$ is solved by substituting the slope k_2 of tangent KQ into Eq. (8):

$$\angle FO_SH = \alpha_2 = 2\pi - \left(\frac{\pi}{2} - \sigma_2\right) - \psi_2 - \theta_2 - \gamma_2$$
$$= \frac{3\pi}{2} + \tan^{-1} k_2 - \psi_2 - \theta_2 - \gamma_2 \quad (8)$$

The length of link FH (namely rod) is obtained in triangle ΔFO_SH by using the law of cosines:

$$|FH| = \sqrt{|O_SF|^2 + |O_SH|^2 + 2|O_SF| \cdot |O_SH| \cdot \cos\angle FO_SH}$$
$$= \sqrt{{l_{21}}^2 + {l_{22}}^2 + 2 \cdot l_{21} \cdot l_{22} \cdot \sin(\tan^{-1} k_2 - \psi_2 - \theta_2 - \gamma_2)} \quad (9)$$

Table 1 Rules of evaluating compensation result

Δey_j^k	Compensation result	Change in deviation
<0	No effect	No change
=0	Adverse effect	Increase in deviation
>1	Over compensation	Significant change caused by a relatively small compensation value
=1	Desired effect	Change equal to the compensation value
<1	Under compensation	Little change caused by a relatively large compensation value

On the basis of the similar analysis conducted for the upper support arm, angle EO_SG and the length of link EG are expressed by Eqs. (10) and (11), respectively.

$$\angle EO_SG = \mathrm{sign}(k_1)\cdot\frac{\pi}{2}-\tan^{-1}k_1+\psi_1-\theta_1-\gamma_1 \tag{10}$$

$$|EG| = \sqrt{{l_{21}}^2+{l_{22}}^2+2\cdot l_{21}\cdot l_{22}\cdot\cos\angle EO_SG} \tag{11}$$

For the alignment of crankshaft, the steady rest should adjust the center O' of crank journal to the center O of headstock as close as possible and thus the displacements of rods EG and FH are given by:

$$\begin{cases} L1_j = |EG|_{(U_O,V_O)}-|EG|_{\left(U_O-Fx_j\cdot dx_j,V_O-Fy_j\cdot dy_j\right)} \\ L2_j = |FH|_{(U_O,V_O)}-|FH|_{\left(U_O-Fx_j\cdot dx_j,V_O-Fy_j\cdot dy_j\right)} \end{cases} \tag{12}$$

Where dy_j and dx_j are the compensation values of crank journal No. j; Fy_j and Fx_j denote the direction in which the corresponding compensation will be applied. If ex_j is a positive number, namely the center of crank journal inclining to the grinding wheel, let Fx_j be −1 to pull the rod EG back. Otherwise, let Fx_j be 1 to push the rod EG forward. If ey_j is a negative number, namely the center of crank journal leaning down to the grinding machine table, let Fy_j be 1 to push the rod FH forward. Otherwise, let Fy_j be −1 to pull the rod FH back.

3 Analysis on the behavior of deviation and the preconditions of automatic alignment

Due to the asymmetric and thus rotating compliance of crankshaft, the support force applied by the steady rest along Y-axis direction changes both X and Y components of deviation and vice versa. According to the results of both simulation and experiment [19], any component of deviation is impacted more greatly by the support force along the direction of component than the support force along its orthogonal direction. Especially, in comparison with the original Y-component deviation, the support force along X-axis generates the change in Y-component deviation just in microns. Considering the alignment precision of large-scale crankshaft and the feasibility of determining compensation values, the interaction of changes in X and Y components of deviation is ignored.

The support force of each steady rest affects the deviations of not only the crank journal to which the force is applied but also the rest of crank journals. The closer the crank journal to the steady rest, the greater the effect appears. It is found by simulation that as for the large-scale crankshaft the support force has a negligible effect on the deviations of the crank journal distant from where the force is exerted [19]. When compensating for the deviation of one crank journal, only the support forces applied to it and to its adjacent ones should be taken into account. In this paper, the steady rests are set up for every other crank journal. And thus, the compensation action can be simplified by considering that the change in deviation of one crank journal supported by steady rest is just caused by the support force directly applied to it.

The support sequence of each steady rest can also influence the change in deviations of crank journals [20]. Besides, the unreasonable support sequence results in the uneven distribution of support forces applied by steady rests. The synchronous control function of CNC system is used here to let all the support pads reach their destinations at the same time.

4 Self-correcting method of compensation

Instead of treating the measured value of deviation as its compensation at first hand, an iterative algorithm is utilized to design the position profile of steady rests with a compromise between accuracy, efficiency, and workpiece surface quality in the traverse grinding [21–23]. A compensation strategy [24] which has good stability and dynamic property in nonlinear system introduced by Tian et al. is employed here to determine the compensation values for the deviation of workpiece axis.

The algorithm for determining compensation value is presented in Fig. 5 where only the equations for Y component are given. All the equations can be adapted for X component by substituting notation 'x' for 'y' during the process of compensation. It is necessary to estimate whether the alignment

Table 2 Radius of crankshaft crank journals in the test experiments

Radius of crank journal R_j (mm)			
j=2	j=4	j=6	j=8
249.400	249.400	249.400	249.160

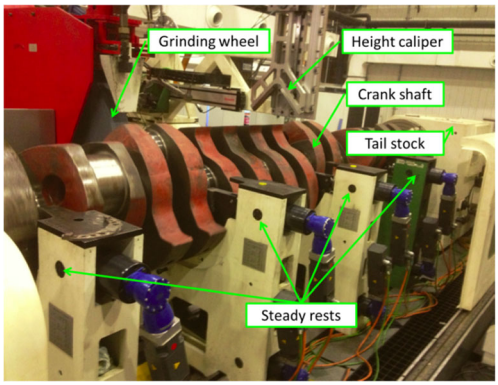

Fig. 6 Grinding machine integrated with the measuring instrument and servo steady rests

precision of crankshaft is achieved or not. If the alignment precision satisfies the conditions that both the maximum deviation $|e_j^k|_{\max}$ and the range of deviation e_{ublb}^k are less than or equal to their expectations, the automatic alignment process ends. This condition constrains not only the peak value but also the difference among the deviations of all the crank journals. The validity of this constraint has been verified by comparing with the conventional one used in the manual alignment process. The algorithm adopts the rules listed in Table 1 to evaluate the compensation result by the value of compensation rate Δey_j^k which is the ratio of the difference between twice deviations before and after compensation and the compensation value used.

When compensation rate Δey_j^k is greater than 1, the compensation value dy_j^{k+1} should be turned down to avoid resulting in the oscillation of deviation. Otherwise, the compensation value dy_j^{k+1} should be turned up to prevent the accumulation of deviation. When compensation rate Δey_j^k is less than zero, let it be zero. Due to the nonlinear performance of the servo steady rest and the measurement noise, the weighted average of the compensation rates $\overline{\Delta ey_j^k}$ in the last t rounds of compensation are substituted for the compensation rate Δey_j^k to determine the compensation regulator q_j^{k+1} for the self-correction of compensation value. The weights P_i of the deviations in the last t rounds are normalized and form a geometric sequence with the common ratio c greater than 1.

Hence, the compensation value for deviation in the next round of compensation can be obtained by the deviation, the average compensation rate, and the compensation regulator of the last round.

Table 3 Parameters of height caliper

Parameters	Values
Length of $\|\boldsymbol{O_HA}\|$ (mm)	337.500
Length of $\|\boldsymbol{O_HB}\|$ (mm)	435.004
Intersection angle of V-block σ (°)	89.950
Initial height $\boldsymbol{H}_0$ (mm)	994.060

Table 4 Parameters of steady rest

Parameters	Values	
	Upper support arm i=1	Lower support arm i=2
$\boldsymbol{l}_{i1}$ (mm)	512.957	546.718
$\boldsymbol{l}_{i2}$ (mm)	382.786	439.659
$\boldsymbol{l}_{i5}$ (mm)	39.990	154.254
$\boldsymbol{\psi}_i$ (°)	43.025	50.194
$\boldsymbol{\theta}_i$ (°)	16.033	146.079
$\boldsymbol{\gamma}_i$ (°)	83.990	66.120
$\boldsymbol{w}_i$ (mm)	100.010	100.012
$\boldsymbol{h}_i$ (mm)	64.508	50.005

5 Case study

To verify the automatic alignment method of the large-scale crankshaft during non-circular grinding, the integrated measuring instrument and four servo steady rests are installed on the grinding machine MK8280SD-H of SMTW. As shown in Fig. 6, four steady rests support the crankshaft of eight throws at its second, fourth, sixth, and eighth crank journals of which the radii are listed in Table 2.

The values of parameters of height caliper needed in the calculation of deviation are listed in Table 3. And the values of parameters used to define the angles and the link lengths of the upper and lower support arms are shown in Table 4. And coordinates (U_O, V_O) of center O of headstock is (249.987, 150.006).

At the start of all the following three alignment tests, the support pads are driven to touch crank journals with the output torque of their servo motors reaching 10 percentages of the maximum value. And the deviations ex_j^0 and ey_j^0 gauged at this moment are used as the initial compensation values in the first round of compensation.

5.1 Test 1: the direct compensation for deviation

The direct alignment test, in which the measured X and Y components of deviation are directly applied to computed the displacements of rods of support arm, is carried out. The measured deviations of four crank journals supported by steady rests after each round of direct compensation are displayed in Fig. 7.

With the progression of direct compensation test, both X and Y components of deviation are approaching to zero at the decreasing rates which nearly reduce to about zero after four rounds of compensation. To some extent, the compensation

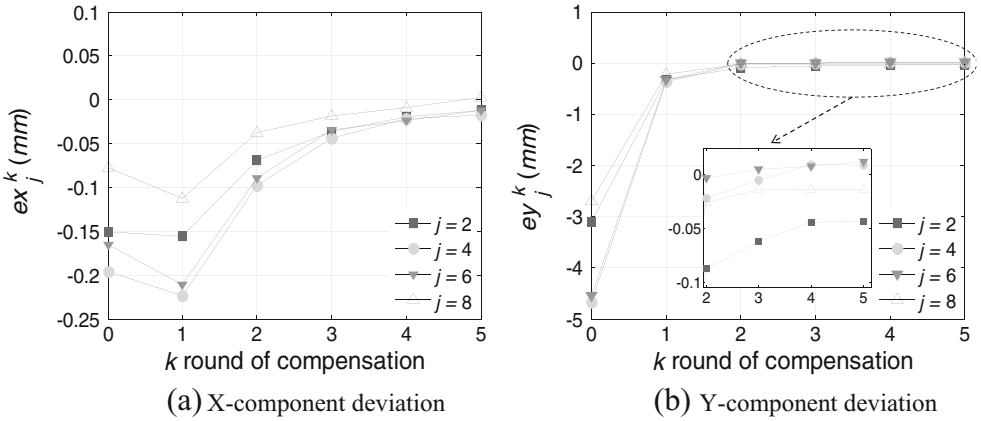

(a) X-component deviation (b) Y-component deviation

Fig. 7 The measured deviation as the result of direct compensation test 1. **a** X-component deviation. **b** Y-component deviation

values of several millimeters for Y-component deviations in the first round of compensation enlarge the X-component deviations as shown in Fig. 8a. However, this effect fades to negligibility as Y-component deviations decrease. After five rounds of compensation, the X-component deviations of all the crank journals drop to 15 μm or so.

For Y component, the compensation rates of the crank journals near the ends of workpiece are lower than the ones in the middle of workpiece. There still exit near 50 μm deviations of the second crank journal while the deviations of middle crank journals reduce to 10 μm after five rounds of compensation. Hence, when the deviations of the fourth and sixth crank journals fall to minute amounts, the overcompensation happens to them easily on account of the still relatively large compensation values for the second and eighth crank journals. In addition, once the direction of the deviations of the fourth and sixth crank journals is opposite to that of the second and eighth ones, the adverse effect of compensation may occur to the two middle crank journals. Thereby, the deviations of the fourth and sixth crank journals are easy to oscillate around 0 while the deviations of the second and eighth crank journals are hard to decrease. This problem can be solved by the self-correction of compensation value discussed in this paper.

5.2 Tests 2 and 3: the self-correcting compensation for deviation

Let the expectation of alignment precision of crankshaft $|e|^*_{\max}$ and e^*_{ublb} equal to 0.025 and 0.03 mm. And let the initial value of compensation regulator q_0, number of compensation round t, and common ratio c be 1, 2, and 3, respectively.

In test 2, 0 is specified for the increment of compensation regulator Δq for both X and Y components. The deviations of the crank journals where the steady rests support after each round of compensation are shown in Fig. 8. Compared with the results of the direct alignment test, not only the maximum X-component deviation is reduced by 16 percentages but also the maximum Y component by 33 percentages after four rounds of compensation. However, the alignment precision of crankshaft listed in Table 5 does not reach its expectation and the rate of compensation drops to near 0 so that the automatic alignment process is manually stopped.

The reasoning of compensation values in each round is revealed in Tables 6 and 7. It can be found that all the compensation rates of X component in the first round are negative as a result of the effect of the large Y-component compensation values up to several millimeters which are over 20 times as large as X-component values. Owing to the negligibility of

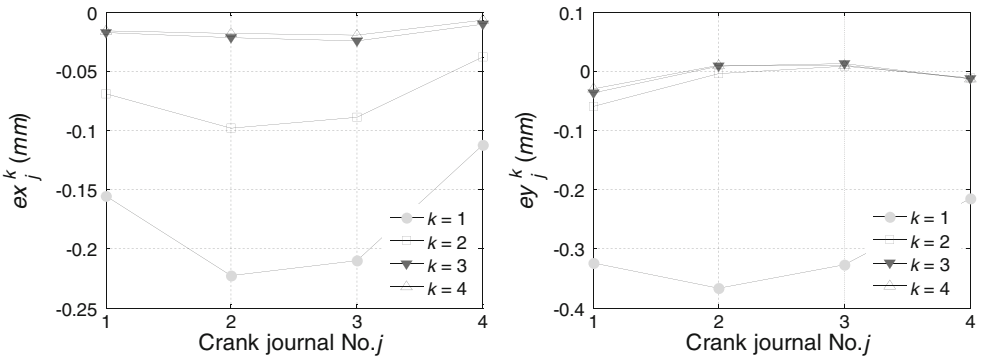

(a) X-component deviation (b) Y-component deviation

Fig. 8 The measured deviation as the result of self-correcting compensation test 2 (Δq=0). **a** X-component deviation. **b** Y-component deviation

Table 5 Alignment precision after each round of two self-correcting compensation tests

Test number	Compensation round k	$\lvert e^k \rvert_{\max}$ (mm)	$e^k_{\mathbf{ublb}}$ (mm)
2	1	0.4287	0.1870
	2	0.0979	0.0707
	3	0.0412	0.0501
	4	0.0335	0.0401
3	1	0.4391	0.1964
	2	0.1033	0.0655
	3	0.0214	0.0284

this effect which results from the decrease of Y-component compensation values, the compensation regulator q_j^1 are set to be 1 for determining X-component compensation values of the next round. Compared with Y component, the X-component deviations are compensated more easily by the enhancement action of compensation regulator, which is due to the small initial values and difference of compensation rates among all the crank journals.

As seen in Table 7, the compensation values for the second and eighth crank journals are heightened by the cooperative action of compensation regulator and average compensation rate. Compared with the result of direction compensation test 1, the self-correcting ability for compensation value of this algorithm reduces the deviation of each main journal into the expectation in the same rounds of compensation, which helps to enhance the efficiency of the automatic alignment process and distribute the support force evenly among all the four steady rests as well.

6 Conclusions

A closed-loop solution with the high efficiency is introduced for precise alignment in non-circular grinding of the large and heavy crankshaft. The discussed approaches and apparatuses can be automated and integrated into the CNC crankshaft grinder and also applied to the practical processing easily.

To achieve the deviation of crank journal axis from the optimum machining axis, an on-machine gauge is proposed. This gauge can measure X and Y components of deviation of crank journal simultaneously. To compensate for the deviation, a servo steady rest driven by motor is introduced to apply support force on the workpieces. The movement of planar linkage in the servo steady rest is analyzed to establish the positional relationship between the pivotable support arm (driven link) and the rod (driving link).

The alignment result is unsatisfied by controlling the positions of support arms according to the measured deviation directly. Therefore, the rules and algorithms for intelligent reasoning of compensation valve are discussed.

A case study of the automatic alignment process is considered to demonstrate this method of determining compensation values. It is seen that a reduction in deviation and an even distribution of support force among the steady rest are achieved in the less rounds of compensation.

The automatic alignment method proposed in this paper shortens the setting-up time and ensures the machining accuracy of large and heavy crankshaft in non-circular grinding.

Table 7 Reasoning of the compensation value for Y-component deviations

Compensation round k	Crank journal No. j	Y axis				
		Δey_j^k	$\overline{\Delta ey_j^k}$	q_j^{k+1}	Fy_j^{k+1}	dy_j^{k+1} (mm)
1	2	0.8940	0.8940	1.3	1	0.4781
	4	0.9200	0.9200	1	1	0.4066
	6	0.9270	0.9270	1	1	0.3573
	8	0.9200	0.9200	1	1	0.2343
2	2	0.6160	0.6855	1.6	1	0.0800
	4	0.9320	0.9290	1	−1	0.0053
	6	0.9675	0.9574	1	−1	0.0151
	8	0.8700	0.8825	1.3	1	0.0173

Table 6 Reasoning of the compensation value of X-component deviations

Compensation round k	Crank journal No. j	X axis				
		Δex_j^k	$\overline{\Delta ex_j^k}$	q_j^{k+1}	Fx_j^{k+1}	dx_j^{k+1} (mm)
1	2	0 (−0.0167)	0	1	1	0.1768
	4	0 (−0.0580)	0	1	1	0.2300
	6	0 (−0.1335)	0	1	1	0.2156
	8	0 (−0.3130)	0	1	1	0.1141
2	2	0.5578	0.4184	1.3	1	0.2429
	4	0.5513	0.4135	1.3	1	0.3245
	6	0.5547	0.4160	1.3	1	0.3000
	8	0.6512	0.4884	1.3	1	0.1059

Since the compensation regulator Δq has a significant impact on the alignment efficiency, further researches will focus on how to settle the appropriate values of Δq for the different sorts of workpiece. In addition, the interaction of each steady rest has to be considered and studied when all the crank journals are supported by steady rests during the grinding of a larger and heavier crankshaft.

Acknowledgments The authors thank the Ministry of Science and Technology of China for National Science and Technology Major Project grant no. 2009ZX04001-111, and also thank for the cooperation of Shanghai Machine Tool Works Ltd.

Compliance with ethical standards This study was funded by the Ministry of Science and Technology of China for National Science and Technology Major Project (grant number 2009ZX04001-111). And this article does not contain any studies with human participants or animals performed by any of the authors. Informed consent was obtained from all individual participants included in the study.

References

1. Fujiwara T, Tsukamoto S, Miyagawa M (2005) Analysis of the grinding mechanism with wheel head oscillating type CNC crankshaft pin grinder. Key Eng Mater 291–292(8):163–168
2. Xu DH, Sun ZY, Zhou ZX, Mi HQ, Wu Y (2002) Research on motion model of tangential point grinding. Chin J Mech Eng 38(8):68–73
3. Möhring HC, Gümmer O, Fischer R (2011) Active error compensation in contour-controlled grinding. CIRP Annals-Manuf Technol 60:429–432
4. Zhou ZX, Luo HP, Xu DH, Sun ZY, Zhou ZX, Mi HQ (2003) Analysis and compensation of stiffness-error of crankshaft in tangential point tracing grinding. Chin J Mech Eng 39(6):98–101
5. Shen NY, He YY, Wu GH, Tian YZ (2006) Calculation model of the deformation due to grinding force in crank pin non-circular grinding. Int Tech Innov Conf: 1325 – 1330
6. Huan J, Ma WM (2010) Method for graphically evaluating the workpiece's contour error in non-circular grinding process. Int J Adv Manuf Technol 46:117–121
7. Yu HX, Xu MC, Zhao J (2015) In-situ roundness measurement and correction for pin journals in oscillating grinding machines. Mech Syst Signal Process 50–51:548–562
8. Claus PK, Daniel H, Hugo T, Bernard G (2008) Process monitoring in non-circular grinding with optical sensor. CIRP Annals-Manuf Technol 57:533–536
9. Hagay B, Hong E, Reuven K, John SA, Susan MS (2012) Non-contact, in-line inspection of surface finish of crankshaft journals. Int J Adv Manuf Technol 60:1039–1047
10. Aaron W (2004) Mathematical modelling of the crankshaft pin grinding process. Dissertation, Deakin University
11. Denkenaa B, Gümmera O (2013) Active tailstock for precise alignment of precision forged crankshafts during grinding. 8th CIRP Conference on Intelligent Computation in. Manuf Eng 12:121–126
12. Cha KC, Wang N, Liao JY (2013) Stability analysis for the crankshaft grinding machine subjected to a variable-position worktable. Int J Adv Manuf Technol 67:501–516
13. Yu GZ, Yu HL, Duan SL (2011) Crankshaft dynamic strength analysis for marine diesel engine. Third Int Conf Meas Tech Mech Autom 1:795–799
14. Jia Z, Xu B, Sun MY, Li DZ, Deng JJ, He MJ (2013) Study on the metal flow of large marine full-fiber crankshaft processed by TR bending up setting method. 11th Int Conf Numer Methods Ind Form Process 1532:812–818
15. Altintas Y, Weck M (2004) Chatter stability of metal cutting and grinding. Ann CIRP 53(2):619–642
16. Jang RS, Sun KL (2002) Machining error compensation of extern cylindrical grinding using a thermally actuated rest. J Mater Proc Technol 127:280–285
17. PG_1106_en_en-US.pdf (2014) http://support.automation.siemens.com/WW/adsearch/resultset.aspx?region=WW&lang=en&netmode=internet&ui=NDAwMDAxNwAA&term=installation+guide+++sinumerik+810&ID=25023768&ehbid=25023768. Accessed 9 March 2014
18. IM8_en_en-US.pdf (2014) http://support.automation.siemens.com/WW/adsearch/resultset.aspx?region=WW&lang=en&netmode=internet&term=HMI&ID=54090527&ehbid=54090527. Accessed 9 March 2014
19. Shen NY, Li J, Wang XD, Ye J, Yu ZX (2014) Analysis and detection of elastic deformation of the large-scale crankshaft in non-circular grinding. Appl Mech Mater 532:285–290
20. Anand R, Shreyes NM (2004) Analysis of the effects of fixture clamping sequence on part location errors. Int J Mach Tools Manufact 44:373–382
21. Gao Y, Jones B (1994) Position motion control of workpiece steadies for compensation in the traverse grinding process. Proc IEEE Conf Control Appl 3:1493–1498
22. Gao Y, Jones B (1993) Control of the traverse grinding process using dynamically active workpiece steadies. Int J Mach Tools Manufact 33(2):231–244
23. Gao Y (1998) Experimental validation of a dynamic workpiece steady control method for traverse grinding. J Manufact Sci Eng 120:236–245
24. Tian XC, Huissoon JP, Xu Q, Peng B (2008) Dimensional error analysis and its intelligent pre-compensation in CNC grinding. Int J Adv Manuf Technol 36:28–33